Supplementary Materials

Supplementary Methods

Cell lines, cell culture and reagents. Doxycycline-inducible human DLBCL cell lines (HBL1, TMD8, U2932, SUDHL2, OCI-Ly10, Toledo, OCI-Ly7, SUDHL4, K422 and OCI-Ly7) that express the bacterial tetracycline repressor were engineered as described previously [48]. Doxycycline (20 ng/ml) was used for inducing the expression of genes of interest. The DLBCL cell lines, Burkitt lymphoma cell lines (Gumbus, Ramos, Raji, BL30, BL70), Hodgkin lymphoma cell lines (L428, L540, L1236) and Jurkat T cells were grown in RPMI 1640 media (Hyclone) supplemented with 20% FBS (fetal bovine serum, Atlanta Biologicals), 100 U/ml penicillin, 100 μg/ml streptomycin (Corning Cellgro), 2 mM GlutaGROTM (Corning Cellgro), 1×MEM-NEAA (Quanlity Biological, Inc.), and 1 mM Sodium Pyruvate Solution (Hyclone). All cultures were routinely tested for mycoplasma contamination. Human embryonic kidney cell line 293T was cultured in DMEM (Dulbecco's modified Eagle's medium, Hyclone) with 10% FBS, 100 U/ml penicillin and 100 μg/ml streptomycin (Corning Cellgro). Cells were treated with AKT inhibitors (AZD5363, Cayman Chemical 1143532-39-1 or AKT inhibitor V (AKTi-V, Triciribine), Selleckchem S1117), and PRMT5 inhibitors (EPZ015666, Cayman Chemical 1616391-65-1 or GSK3326595, Chemietek CT-GSK332) when needed. All cell lines were cultured at 37°C in a 5% CO2 atmosphere.

EPZ015666 is an S-adenosylmethionine (SAM) cooperative inhibitor of PRMT5 that binds at the peptide binding site of PRMT5 (1,2). The selectivity had been tested against a panel of 20 other protein methyltransferases, showing no inhibition up to the maximum tested concentration of 50 μM (1). The more potent PRMT5 inhibitor, GSK3326595, is being used for two phase I trials (NCT02783300, NCT03614728) in the solid tumors, non-Hodgkin lymphoma and leukemia (3).

AZD5363, an ATP competitive inhibitor (4), inhibits all forms of AKT (AKT1/2/3) and other members in the AGC family (5) as they share a high degree of sequence similarity in the catalytic domain. AKT inhibitor V (AKTi-V), an allosteric inhibitor of AKT, binds to the N terminal PH domain of AKT and blocks its recruitment to the cell membrane (6). AKTi-V inhibits AKT1, AKT2 and AKT3, and it is highly selective for AKT over PKC, PKA and SGK, 3 members in the AGC family that are closer to AKT kinase than other members (7). Both AKT inhibitors are in clinical trials (8,9).

Gene knockout with an inducible 2-vector CRISPR-Cas9 knockout system. pRSGT16-U6Tet-sg-HTS6C-CMV-TetRep-2A-TagRFP-2A-Puro (Cellecta) was used for generating sgRNA targeting specific gene and pR-CMV-Cas9-2A-Hygro (Cellecta) for generating Cas9-expressing cells. We first introduced Cas9 expressing plasmid into different DLBCL cell lines via lentiviral transduction. After hygromycin selection, Cas9 expression cells were diluted and seeded onto 96-well plates. Single-cell clones were confirmed by light microscope (ZEISS Primo Vert). For each cell line we chose the clone that has the highest expression level of Cas9 as confirmed by immunoblot with Cas9 antibody (EMD Millipore, MAC133). High expression of Cas9 can guarantee the knockout efficiency. To knockout the gene of interest, we designed sgRNA seed sequence using online software (https://chopchop.rc.fas.harvard.edu/), and inserted the sequence into sgRNA construct following the manufacturer's instructions. After introducing sgRNA targeting a specific gene into Cas9 expression clones, cells were selected by puromycin. Then doxycycline was used to induce the expression of sgRNA and the subsequent knockout of the target gene. The following seed sequences were used for knockout of PRMT5, BTK and p65:

PRMT5: AGAGGCCAATGGTATATGAG
BTK: GATGCTCTCCAGAATCACTG
RELA: GACCCCGGCCATGGACGGTG

PRMT5 plasmid construction. The Flag-PRMT5 cDNA (a gift from Dr. Stephen Nimer's group) was subcloned into BamH1 and Xho1 restriction sites of the retroviral pCMVTO-eGFP-hygro vector using the following primers:
Forward: TCTATGTATAGGATCCGCCACCATGGACTACAAGGACGACGATGACAAGATGG CGGCGATGGCGGTCGGG
Reverse: TCTATGTATACTCGAGCTAGAGGCCAATGGTATATGAGCG

Immunoblotting assay. Cells were lysed using MAPK lysis buffer (50 mM HEPES, 4 mM sodium pyrophosphate, 10 mM sodium fluoride, 2 mM orthovanadate, 100 mM NaCl, 10 mM EDTA, pH 7.5) with protease inhibitor cocktail (Sigma). Protein concentrations were determined by BCA assay (Thermo Scientific). Proteins were separated by SDS-PAGE and transferred to nitrocellulose membranes. After blocking with non-fat milk, the membrane was probed with primary antibodies against proteins of interest. The primary antibodies included anti-PRMT5 (EMD Millipore EPR 5772), anti-symmetrically dimethylated Histone 4 R3 (Abcam ab231658), anti-PRMT7 (Santa Cruz Biotechnology sc-166189), anti-PRMT9 (EMD Millipore MABE 1112), anti-BTK (Cell Signaling Technology 8547), anti-NF-kB p65 (Cell Signaling Technology 8242), anti-E2F1 (Cell Signaling Technology 3742), anti-RBL2 (Cell Signaling Technology 13610), anti-β-actin (Cell Signaling Technology 4967), anti-phospho-GSK3β (Cell Signaling Technology 9323), anti-AKT (Cell Signaling Technology 2920), anti-phospho-AKT (Cell Signaling Technology 9271), anti-IRF4 (Santa Cruz Biotechnology sc-6059), anti-MYC (Abcam 32072) and anti-p53 (Cell Signaling Technology 9282). After blotting with the HRP-conjugated secondary antibody, the membrane was developed using a chemiluminescence HRP substrate kit (Thermo Scientific).

Cell cycle analysis. Cell cycle was analyzed with BD Pharmingen™ BrdU Flow Kits (Cat#: 552598). Briefly, cells were pulsed with BrdU for 3 hrs, followed by fixation and permeabilization procedures. Then, the cells were stained with APC-conjugated anti-BrdU antibody, followed by 7-AAD staining for the total amount of DNA. Cells were then analyzed on a MACS Quant10 flow cytometer (Miltenyi Biotec). DNA contents were analyzed using FlowJo software (FlowJo, LLC).

Cell viability assay. Cells were seeded onto 96-well plates**.** For trypan blue exclusion cell viability assay, the total number of viable cells was counted every 3 days. For each counting, 10 μl of the cell suspension was loaded onto TC20 system (Bio-Rad) counting slides. Cell viability was measured with an automatic cell counter according to the manufacturer's instructions. For CellTiter-Glo™ Luminescent Cell Viability Assay, cell viability was measured using CellTiter-Glo® 2.0 Assay (Promega, G9242) following manufacturer's instructions. Luminescence signal was read using ENSPIRE plate reader (PerkinElmer).

Naive B cell isolation. Naive human B cells were isolated from peripheral blood mononuclear Cells (PBMCs) or human tonsils using naive B cell isolation kit (Miltenyi Biotec) according to the manufacturer's instructions. All tissues were collected with institutional review board (IRB) approval (Protocol #2013-1570, #2015-1483) by the University of Wisconsin-Madison. Briefly, mononuclear cells were isolated by density gradient centrifugation, and red blood cells were lysed with ACK lysing buffer. Naive B cell biotin-antibody cocktail was then added and incubated for 5 min at 4 °C. After incubation, anti-biotin microbeads were added and incubated for additional 10 min at 4 °C. Negative selection was then performed by an AutoMACS Pro (Miltenyi Biotec). The purity was measured by

FITC-CD20 (clone: LT20, Miltenyi Biotec) and PE-CD27 (clone O323, eBiosciences) staining (~98%).

Immunohistochemical staining and quantification. To study PRMT5 and BTK expression in DLBCL, tissue microarrays were constructed from archival cases of *de novo* DLBCLs diagnosed at Indiana University Health Pathology Laboratory during 2000-2014, with approval from the Indiana University IRB (Protocol#1407470378). DLBCL TMAs were stained for CD3 (Dako clone IR503), CD20 (Dako clone IR604), CD10 (Dako clone IR648), BCL-6 (Dako clone IR625), and MUM-1 (Dako clone IR644) for classification of GCB and Non-GCB subtypes. The antibodies PRMT5 (Abcam ab31751), and BTK (Cell Signaling Technology 8547) were used. A tissue microarray (TMA) of mantle cell lymphoma cases was obtained from our previous study (10), with approval from the University of Wisconsin-Madison Institutional Review Boards (UW protocol M-2008-1011 and MCRF protocol SHA 10109). Protein expression was scored using InformTM advanced image analysis software. Scores of duplicated cores were averaged for each case.

Xenografts. Male and female NOD.Cg-Prkdcscid Il2rgtm1Wjl/SzJ (NSG) breeder pairs were purchased from The Jackson Laboratory (Bar Harbor, ME, USA) and bred under specific pathogen-free conditions in sterile ventilated racks in the animal care facility at the University of Wisconsin-Madison. All animal protocols were approved by the Animal Care and Use Committee. NSG male and female mice were used between 8-16 weeks of age. Live TMD8 and OCI-Ly7 cells expressing inducible sgPRMT5 at 1×10^7 cells were resuspended in 0.2 ml sterile PBS and injected subcutaneously (s.c) into previously shaved right flanks of female and male NSG mice. Tumor growth was measured by digital caliper in two orthogonal dimensions. When tumors were palpable (~5mm), mice were randomized into treatment groups such that each group started with matching tumor sizes. Doxycycline was added to the drinking water of one group of mice to induce knockout of PRMT5. Tumor measurements were recorded 3 times a week, and volumes were calculated as previously described (11). When mice became moribund or when tumors exceeded 20 mm in any direction, mice were euthanized as required by institutional protocols.

DLBCL patient derived xenografts (PDX). DLBCL PDX model was established as described previously (12). All experimental procedures and protocols (the animal IACUC protocol # 00001260 and the tissue collection protocol# Lab11-0342) were approved by the Institutional Animal Care and Use Committee and Institutional Review Boards of The University of Texas MD Anderson Cancer Center. Briefly, 10-week-old male NSG mice were housed in the animal research facility. 5×10^6 freshly isolated DLBCL cells were directly injected into the fetal bone chip of NSG-hu mice after the mice were anesthetized with 5% isoflurane vaporizer. Once tumor growth was detected in the first generation, tumor mass was monitored and then passaged. The passaged tumor equally grew and mice were assigned as 5 mice/group for *in vivo* treatment. Three days after tumor implantation, the mice were administered vehicle control or GSK3226595 100mg/kg, oral gavage, twice per day for 35 consecutive days. Tumor burden was evaluated by measuring tumor volume using a formula volume $(v) = a \times b^2/2$ (a: long diameter; b: short diameter). Survival time was calculated from treatment day to endpoint (one diameter of tumor mass reaches 15 mm or when mouse become moribund).

Chromatin Immunoprecipitation (ChIP) assay. ChIP assay was performed using Simplechip Plus Enzymatic Chromatin IP Kit (Cell Signaling Technology 9003s) according to the manufacturer's instructions. Briefly, 10×10^6 cells with or without the knockout of specific genes were fixed with formaldehyde for 10 min at room temperature. The cross-linking reaction was stopped by addition of 1× glycine solution for 5 min. Cells were washed twice with ice-cold PBS. Pellets were lysed, and

digested with micrococcal nuclease for 20 min at 37°C, and then sonicated 20s on, 30s off for nine cycles using a cup horn sonicator (qsonica #Q500-110) at 4°C. DNA fragments were recovered using anti-p65 (Cell Signaling Technology#8242), anti-cMyc (Santa Cruz Biotechnology sc-40X), normal rabbit anti-IgG or normal mouse anti-IgG (sc-2025). Recovered DNA fragments were directly used for real-time PCR analysis with specific primers. The promoter region of human PRMT5 was amplified from immunoprecipitated genomic DNA with the following primers:
PRMT5-p65-F: 5'-CATCTTTCTCCTCGCGCTGT-3'
PRMT5-p65-R:5'- GGTGGATCCATGCCGTACGC-3'
PRMT5-myc-F: 5'-AACAGGAGGGATGGGGAGTG-3'
PRMT5-myc-R: 5'-CTCCGTGATGGTACTTCAAG-3'
The SensiFAST™ SYBR® Hi-ROX Kit (Bioline BIO-92020) was used for qPCRSupplementarl reaction.

RNA-seq analysis. Total RNA was extracted using RNeasy plus mini kit (Qiagen) according to the manufacturer's protocol. RNA-seq libraries were prepared by using the Illumina TruSeq stranded mRNA LT sample preparation kit (Illumina). Sequencing was performed on Illumina Hiseq 2500 at 50-bp length. For the RNA analysis, raw reads were mapped to the human reference genome (UCSC hg19) by HISAT2 (v2.1), and differential expression analysis was done by StringTie (v1.3.4) and Ballgown [53]. Gene ontology analysis was performed by Panther Classification System (http://pantherdb.org/). Gene Set Enrichment Analysis (GSEA) was performed by GSEA software (V2.0) (http://software.broadinstitute.org/gsea/index.jsp). For the GSEA analysis, molecular signatures databases h.all.v5.2 symbols.gmt was used. RNAseq data discussed in this publication have been deposited in the National Center for Biotechnology Information's Gene Expression Omnibus and are accessible through GEO Series accession number: GSE115136.

Statistical analysis. Two-tailed Student's *t*-test was used to determine a significant difference. Results were presented as mean ± standard deviation (SD). *P < 0.05, **P < 0.01, and ***P < 0.001 were used to show statistical significance.

Supplementary References

1. Chan-Penebre E, Kuplast KG, Majer CR, Boriack-Sjodin PA, Wigle TJ, Johnston LD, et al. A selective inhibitor of PRMT5 with in vivo and in vitro potency in MCL models. *Nat Chem Biol.* 2015 Jun;11(6):432–7.
2. Duncan KW, Rioux N, Boriack-Sjodin PA, Munchhof MJ, Reiter LA, Majer CR, et al. Structure and Property Guided Design in the Identification of PRMT5 Tool Compound EPZ015666. *ACS Med Chem Lett.* 2016 Feb 11;7(2):162–6.
3. Inc E. Epizyme Earns $6 Million Milestone Payment from GlaxoSmithKline for Initiation of Clinical Development with First-in-Class PRMT5 Inhibitor [Internet]. GlobeNewswire News Room. 2016 [cited 2019 Feb 1]. Available from: *http://globenewswire.com/news-release/2016/09/15/872059/0/en/Epizyme-Earns-6-Million-Milestone-Payment-from-GlaxoSmithKline-for-Initiation-of-Clinical-Development-with-First-in-Class-PRMT5-Inhibitor.html*
4. Addie M, Ballard P, Buttar D, Crafter C, Currie G, Davies BR, et al. Discovery of 4-amino-N-[(1S)-1-(4-chlorophenyl)-3-hydroxypropyl]-1-(7H-pyrrolo[2,3-d]pyrimidin-4-yl)piperidine-4-carboxamide (AZD5363), an orally bioavailable, potent inhibitor of Akt kinases. *J Med Chem.* 2013 Mar 14;56(5):2059–73.

5. Davies BR, Greenwood H, Dudley P, Crafter C, Yu D-H, Zhang J, et al. Preclinical pharmacology of AZD5363, an inhibitor of AKT: pharmacodynamics, antitumor activity, and correlation of monotherapy activity with genetic background. *Mol Cancer Ther.* 2012 Apr;11(4):873–87.
6. Berndt N, Yang H, Trinczek B, Betzi S, Zhang Z, Wu B, et al. The Akt activation inhibitor TCN-P inhibits Akt phosphorylation by binding to the PH domain of Akt and blocking its recruitment to the plasma membrane. *Cell Death Differ.* 2010 Nov;17(11):1795–804.
7. Yang L, Dan HC, Sun M, Liu Q, Sun X, Feldman RI, et al. Akt/protein kinase B signaling inhibitor-2, a selective small molecule inhibitor of Akt signaling with antitumor activity in cancer cells overexpressing Akt. *Cancer Res.* 2004 Jul 1;64(13):4394–9.
8. Brown JS, Banerji U. Maximising the potential of AKT inhibitors as anti-cancer treatments. *Pharmacol Ther.* 2017 Apr;172:101–15.
9. NITULESCU GM, MARGINA D, JUZENAS P, PENG Q, OLARU OT, SALOUSTROS E, et al. Akt inhibitors in cancer treatment: The long journey from drug discovery to clinical use (Review). *Int J Oncol.* 2015 Dec 24;48(3):869–85.
10. Li Y, Wang F, Lu L, Zhu F, Huang S, Nomie K*, et al.* NR4A1 inhibition synergizes with ibrutinib in killing mantle cell lymphoma cells. *Blood cancer journal* 2017 Nov 23; **7**(12)**:** 632.
11. Li Y, Bouchlaka MN, Wolff J, Grindle KM, Lu L, Qian S*, et al.* FBXO10 deficiency and BTK activation upregulate BCL2 expression in mantle cell lymphoma. *Oncogene* 2016 Dec 1; **35**(48)**:** 6223-6234.
12. Zhang L, Nomie K, Zhang H, Bell T, Pham L, Kadri S*, et al.* B-Cell Lymphoma Patient-Derived Xenograft Models Enable Drug Discovery and Are a Platform for Personalized Therapy. *Clinical cancer research : an official journal of the American Association for Cancer Research* 2017 Aug 1; **23**(15)**:** 4212-4223.

Supplementary Figure Legends

Figure S1. PRMT5 expression in mantle cell lymphoma cases and lymphoma cell lines. (A) Immunohistochemical analysis of PRMT5 expression in 31 mantle cell lymphoma patient tumor tissues and 5 human tonsils and 6 lymph nodes, analyzed with InformTM advanced image analysis software (student's *t*-test, **p<0.01). (B) Immunoblot analysis of PRMT5 expression in the indicated Burkitt lymphoma (BL) cell lines, Hodgkin lymphoma cell lines (HL) and Jurkat T cells (relative to OCI-Ly1). β-actin served as a loading control.

Figure S2. Knockout of BTK, RELA and MYC reduces PRMT5 expression. (A) BTK sgRNA expression does not affect the expression levels of PRMT5 in GCB DLBCL. OCI-Ly7 and SUDHL4 cells expressing sgRNA targeting BTK were seeded into 96-well plates and single cell clones were selected. Shown are representative clones for each cell line. (B-D) Immunoblot analysis shows a time-dependent reduction of PRMT5 expression after induction of expression of sgBTK (B), sgRELA (C) or sgMYC (D) with 20 ng/ml doxycycline. (E) Trypan blue dye exclusion viability assay of the indicated cell lines after 6 days of induction of sgRELA or sgMYC with 20 ng/ml doxycycline.

Figure S3. Apoptosis analysis after inhibition of AKT with AZD5363. Cells were treated with 1 μM AZD5363 for 3 days before flow cytometric analysis of apoptosis.

Figure S4. Apoptosis analysis after inhibition of PRMT5. (A) Titration of the PRMT5 inhibitor EPZ015666 in HBL1, Granta-519, and Jeko cell lines by trypan blue dye exclusion viability assay. Error bars represent mean ± SD (*p<0.05, n=3). (B) Cell cycle analysis of HBL1, OCI-Ly10, OCI-Ly1 and K422 cells after 6 days of treatment with 1 μM EPZ015666. Error bars represent mean ± SD (*p<0.05, **p<0.01, N=3). (C) Proliferation of naive B cells was not affected by the PRMT5 inhibitor when stimulated with 10 mg/ml anti-IgM. Error bars represent mean ± SD (N =3). (D) Inhibition of PRMT5 with 1 μM of EPZ015666 for 6 days in TMD8 and OCI-Ly1 cells or (E) by induction of PRMT5 sgRNA for 6 days in TMD8 and HBL1 cells.

Figure S5. PRMT5 cDNA expression rescues the cytotoxicity of PRMT5 sgRNA and PRMT5 sgRNA reduces cell proliferation. (A) HBL1 and OCI-Ly7 cells stably expressing sgPRMT5 or sgPRMT5 together with Flag-tagged PRMT5 were induced with doxycycline for 6 days. Cell viability was measured with trypan blue dye exclusion assay and normalized to uninduced cells. Error bars represent mean ± SD (*p<0.05, n=3). (B) Cell cycle analysis of TMD8 and OCI-Ly7 cells after 6 days of PRMT5 sgRNA induction. Error bars represent mean ± SD (*p<0.05, ** p<0.01, N=3).

Figure S6. RNA-seq analysis in DLBCL cell lines after PRMT5 knockout. (A) Immunoblot analysis of PRMT5 expression after 3 days or 5 days of PRMT5 sgRNA induction in TMD8 and OCI-Ly7 cells. (B) Venn diagrams show upregulated and downregulated genes in TMD8 and OCI-Ly7 cells. (C) Gene set enrichment analysis (GSEA) of glycolysis and cholesterol homeostasis signature genes in TMD8 and OCI-Ly7 cells. (D) GSEA between germinal center B cells (n=4) and naive B cells (n=4) based on published RNA-seq data (Beguelin, et al., *Cancer Cell*. 2016; 30(2): 197-213).

Figure S7. PTEN expression reduces sensitivity of DLBCL cells to the AKT inhibitor AZD5363. (A) Immunoblot analysis of PTEN expression in the indicated DLBCL cell lines. β-actin served as a loading control. (B) Titration of AZD5363 in the indicated DLBCL cell lines by CellTiter-Glo™ Luminescent Cell Viability Assay.

Figure S8. PDX and cytogenetic analysis of DLBCL patients. (A) There was no change of the mouse body weight with GSK3326595 treatment. Body weight were calculated during drug treatment (GSK3226595 vs vehicle, p=0.637). (B) Fish cytogenetic analysis of MYC, BCL-2 and BCL-6 translocation with immunoglobulin genes.

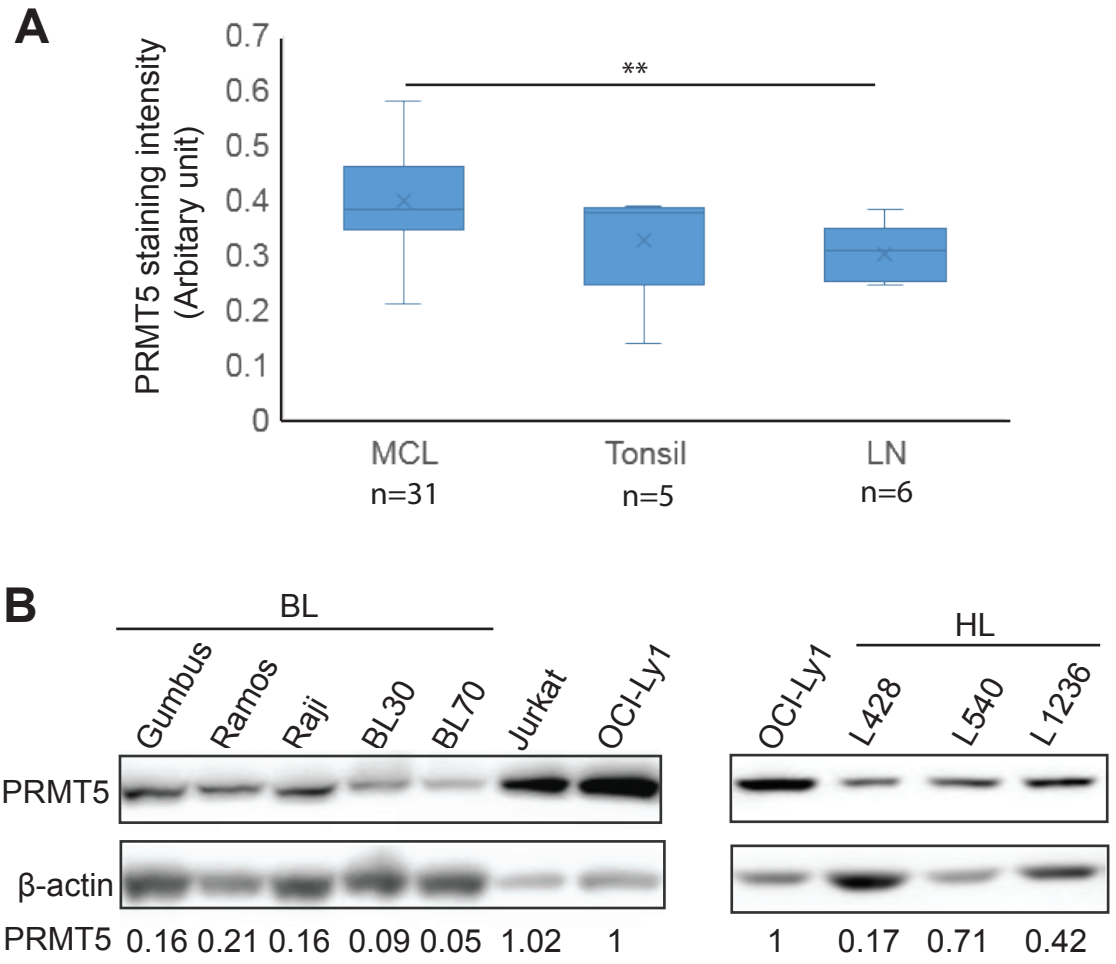

Supplementary Figure 1

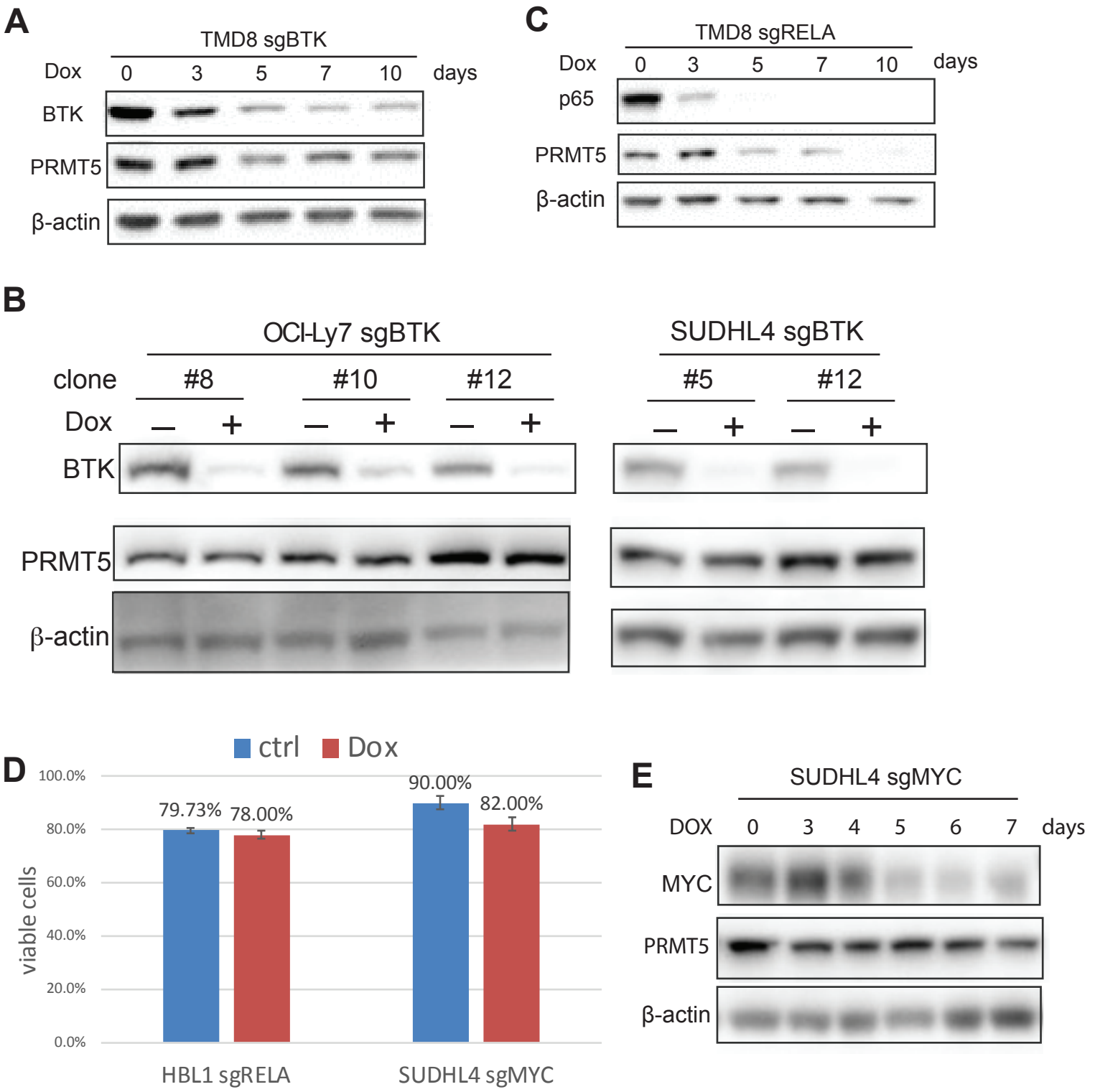

Supplementary Figure 2

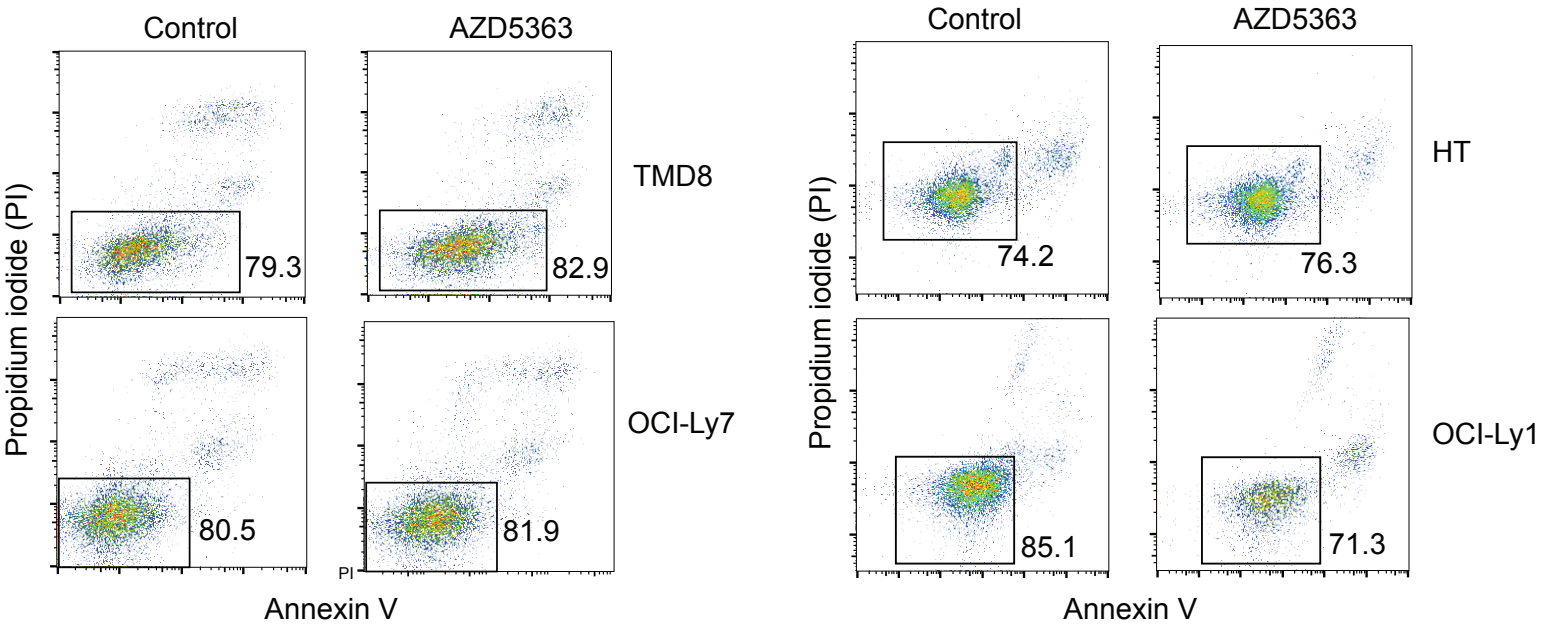

Supplementary Figure 3

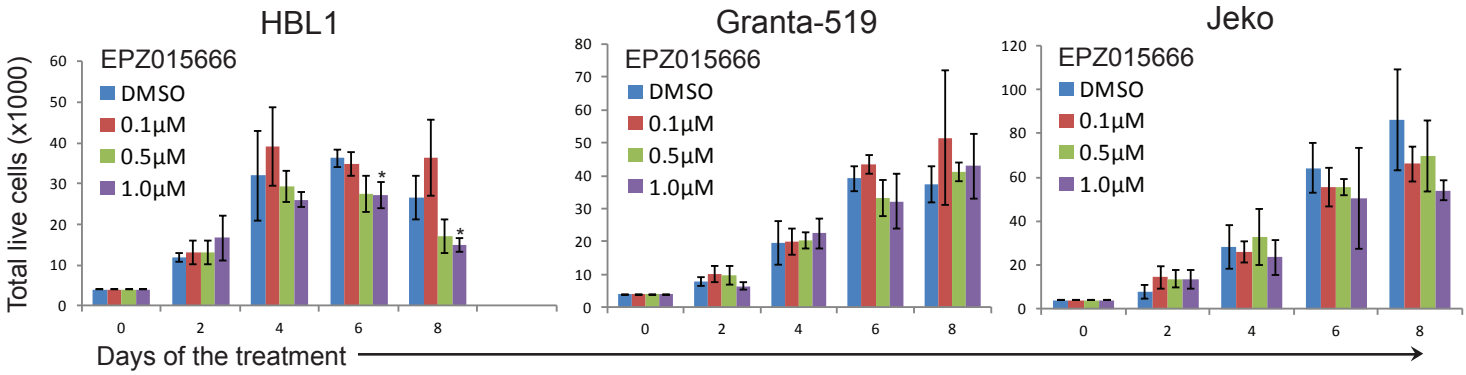

B

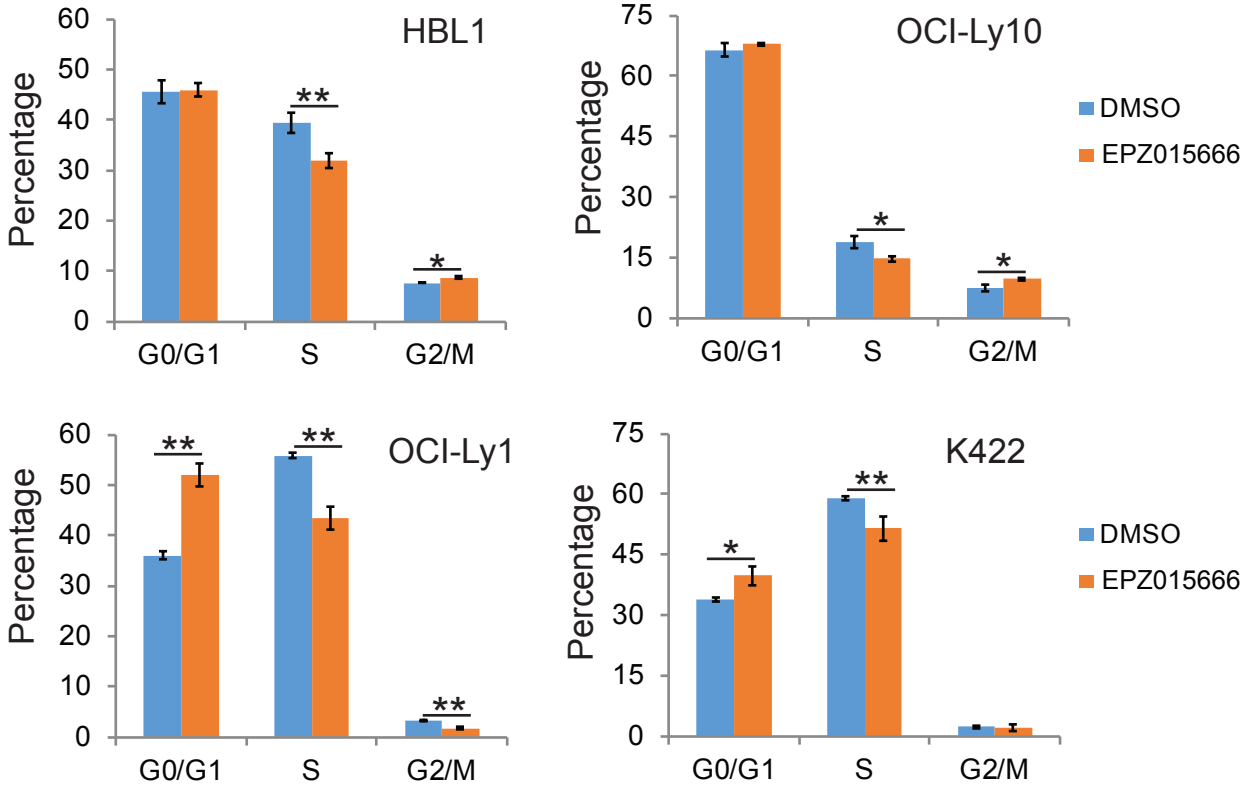

C

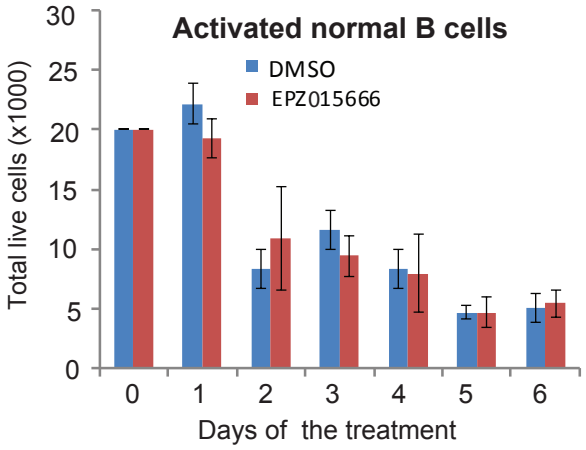

D

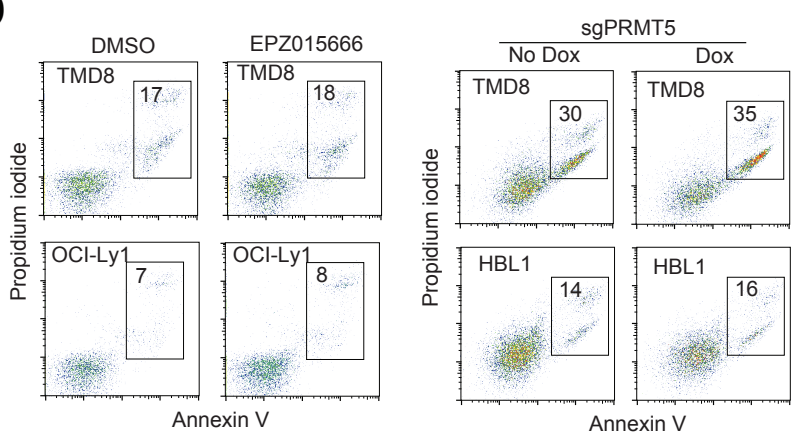

Supplementary Figure 4

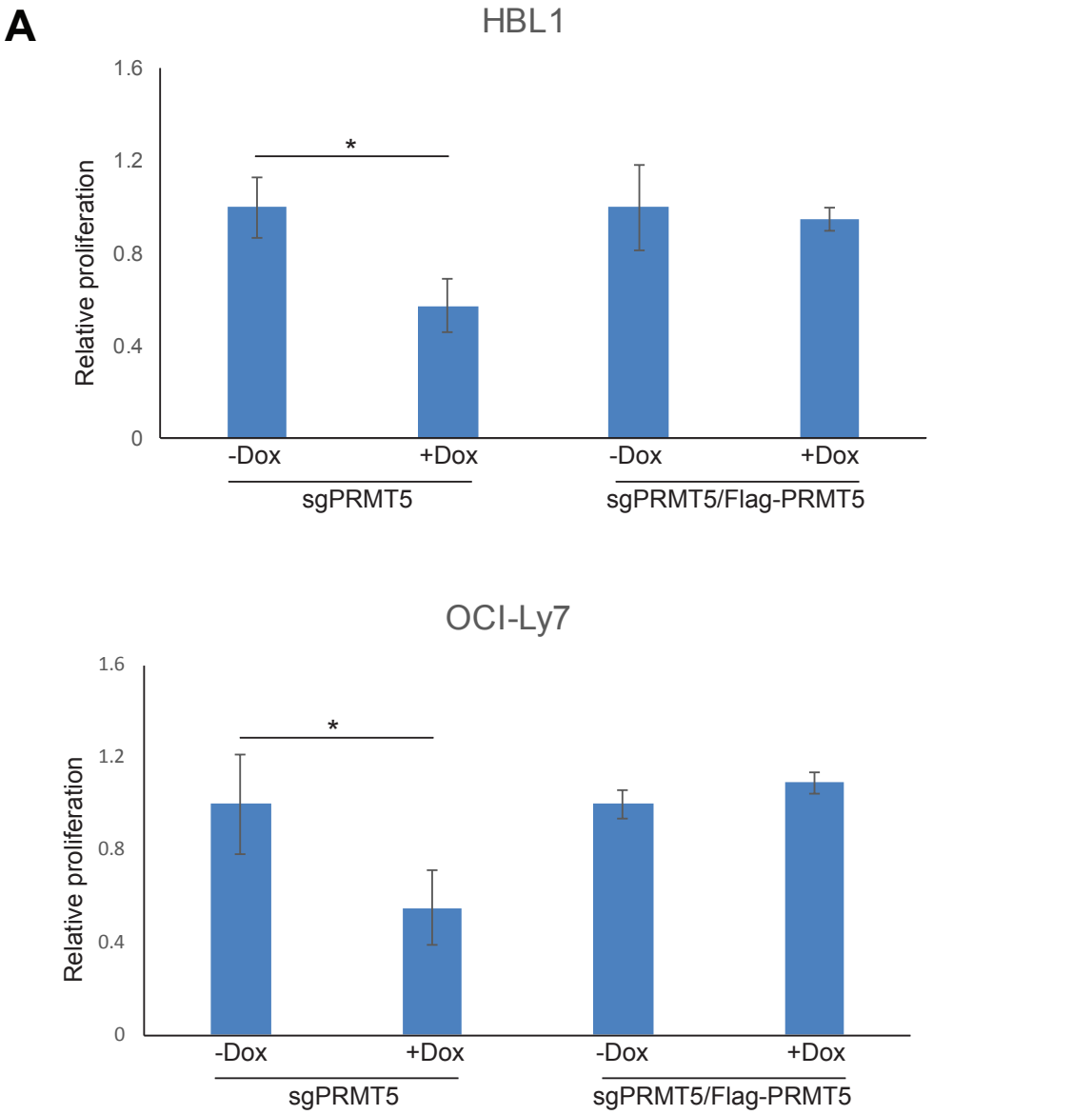

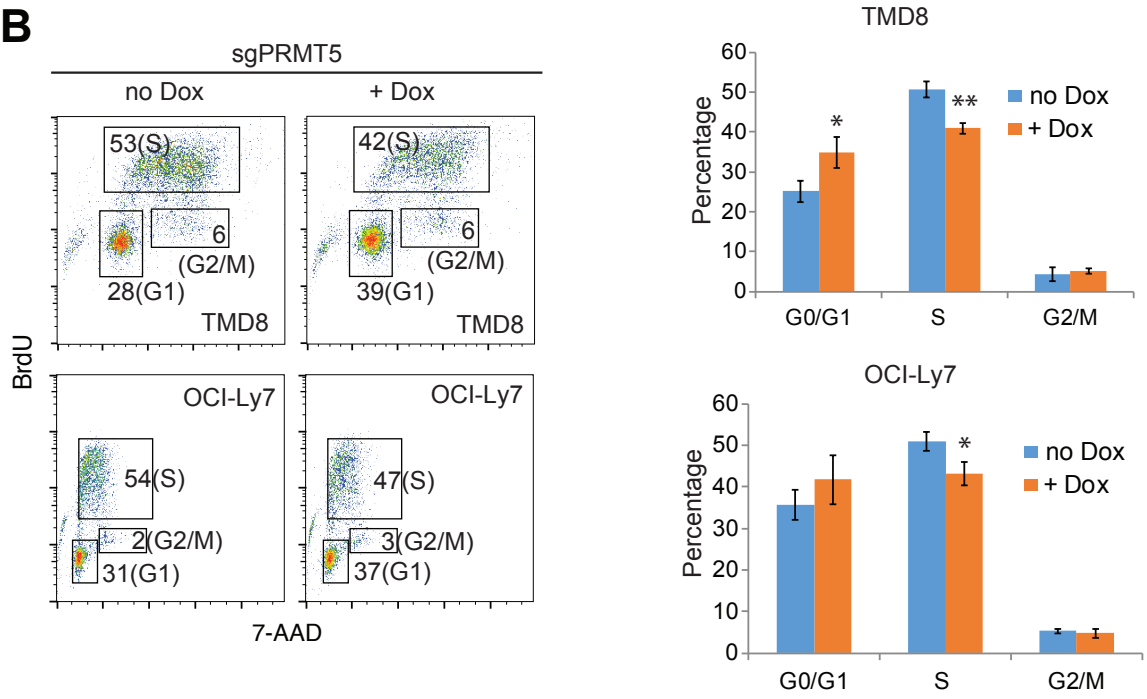

Supplementary Figure 5

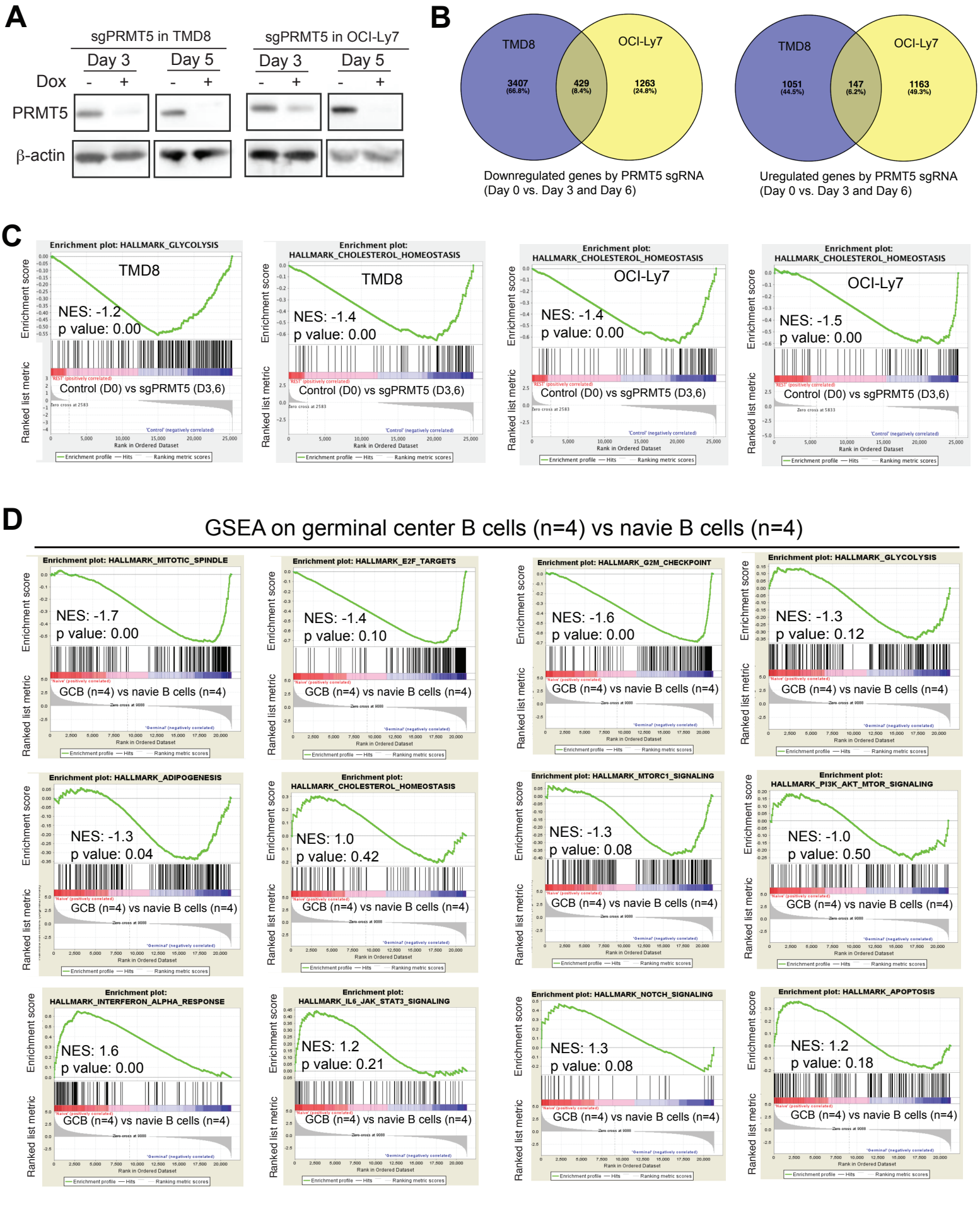

Supplementary Figure 6

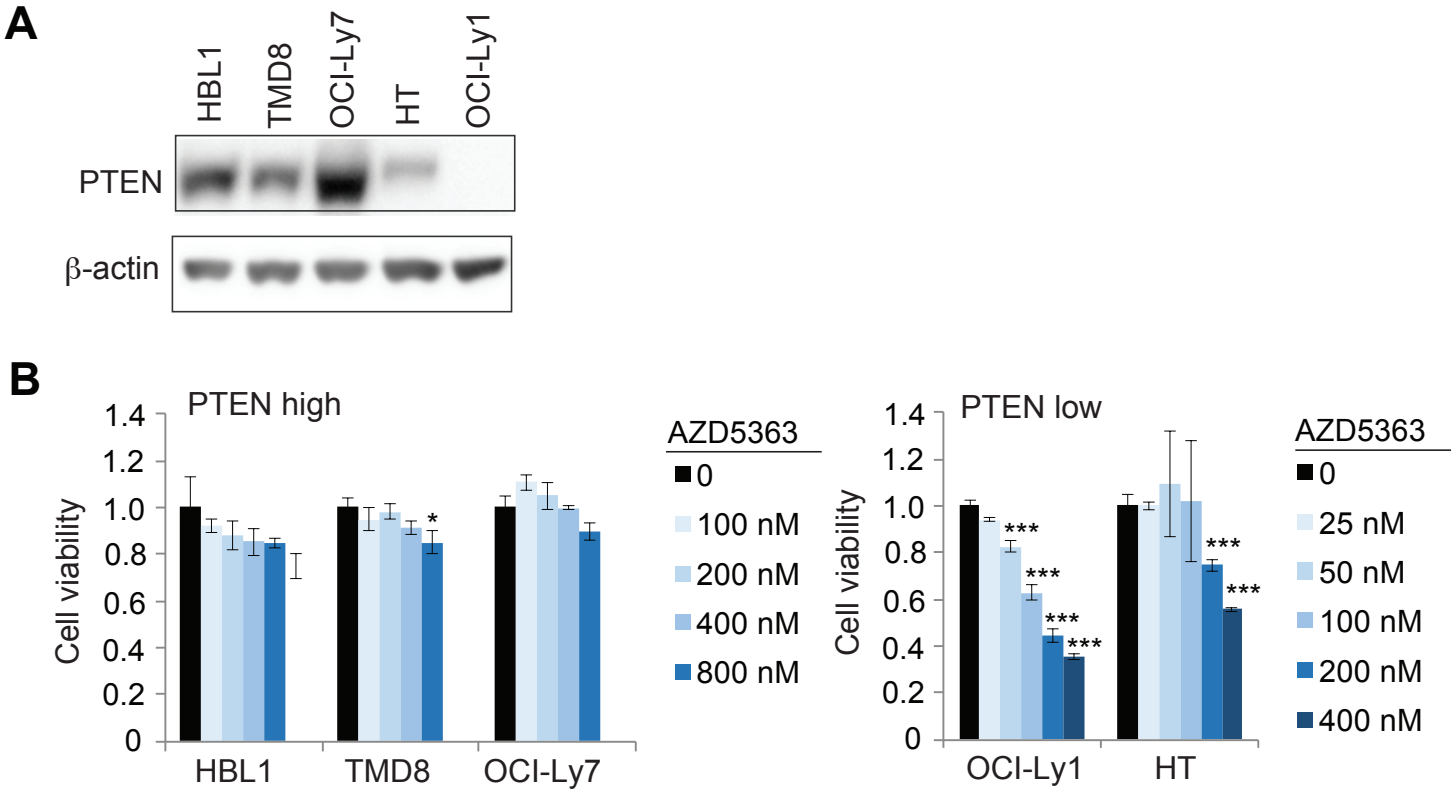

Supplementary Figure 7

A

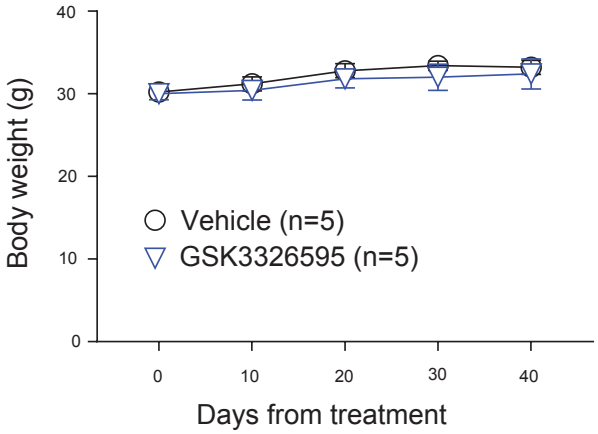

B

Cytogenetic analysis of gene arrangement

DLBCL	Type	MYC	BCL-2	BCL-6
PT1	GCB	+	-	-
PT2	DIT	+	+	-
PT3	ABC	-	-	-

Supplementary Figure 8